

# Effect of sodium montmorillonite nanoclay on the water absorbency and cationic dye removal of carrageenan-based nanocomposite superabsorbents

Gholam Reza Mahdavinia · Bakhshali Massoumi · Karim Jalili · Gholamreza Kiani

Received: 16 February 2012 / Accepted: 24 July 2012 / Published online: 7 August 2012  
© Springer Science+Business Media B.V. 2012

**Abstract** Nanocomposite superabsorbents were synthesized by simultaneously solution copolymerization of acrylamide (AAm) and sodium acrylate (Na-AA) in the presence of carrageenan biopolymer and sodium montmorillonite (Na-MMt) nanoclay. Potassium persulfate (KPS) and methylenebisacrylamide (MBA) were used as initiator and cross-linker, respectively. The structure and morphology of the nanocomposites were investigated using XRD, FTIR, scanning electron microscopy (SEM), and TEM techniques. The influence of nanoclay and carrageenan contents as well as monomer weight ratios on the degree of swelling of nanocomposites was studied. The optimum water absorbency was obtained at 10 wt% of clay, 10 wt% of carrageenan, and 1:1 of monomers weight ratio. The obtained nanocomposites were examined to remove of crystal violet (CV) cationic dye from water. The effect of carrageenan and clay content on the speed of dye adsorption revealed that while the rate of dye adsorption is enhanced by increasing the clay content up to 14 wt% of clay, it was decreased as the carrageenan increased in nanocomposite composition. The results showed that the pseudo-second-order adsorption kinetic was predominated for the adsorption of CV onto nanocomposites. The experimental equilibrated adsorption

capacity of nanocomposites was analyzed using Freundlich and Langmuir isotherm models. The results corroborated that the experimental data fit the Freundlich isotherm the best.

**Keywords** Superabsorbent · Nanocomposites · Carrageenan · Removal · Cationic dye

## Introduction

Superabsorbents are type of three-dimensional hydrophilic polymers capable to swell and absorb a large amount of water [1]. They are mainly used in sanitary goods for absorbing the body fluids and in soil conditioning and improving the water retention capability of soil in agriculture and horticulture [2]. They are also found to be valuable in some specialized applications, including controlled delivery of bioactive agents [3] and wastewater treatment [4]. Superabsorbents can be classified into non-ionic and ionic materials. The ionic types comprise anionic ( $-\text{CO}_2^-$ ,  $-\text{SO}_3^-$ ) or cationic pendants ( $-\text{NR}_3^+$ ) [5]. The presence of these ionic groups in the superabsorbents opens potential area of application that is related to remove of pollutants from wastewaters [6]. Industry is a huge source of water pollution; it produces pollutants that are excessively harmful to people and the environment. Colored water and solutions containing toxic heavy metals from many industries like dye, textile, paper, plastic, plating, and mining facilities produce considerable polluted waters. The pollutions must be removed from wastewater before discharging it into the environment. Adsorption process, an inexpensive and simple design, can be used to remove of dye contaminations from aquatic environments [7]. The colors pollutants are anionic or cationic molecules. The existence of anionic and cationic pendants in the superabsorbents makes them to show

G. R. Mahdavinia (✉)  
Department of Chemistry, Faculty of Science,  
University of Maragheh,  
P.O. Box 55181-83111, Maragheh, Iran  
e-mail: grmnia@maragheh.ac.ir

B. Massoumi · K. Jalili  
Department of Chemistry, Faculty of Science,  
Payame Noor University,  
P.O. Box 19395-3697, Tehran, Iran

G. Kiani  
School of Engineering-Emerging Technologies, Tabriz University,  
Tabriz, Iran

complexing ability with materials with opposite charges. So, anionic and cationic superabsorbents have been used to remove of anionic and cationic dyes from aquatic media [8, 9]. Similarly to the dye removal, the adsorption of heavy metal cations by anionic pendant of superabsorbents is another capability of these materials [10].

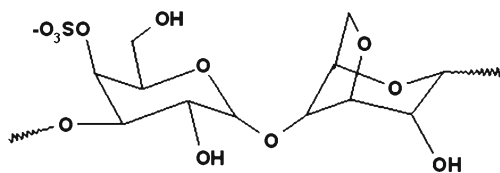
But, these superabsorbents mainly do not possess adequate strength. Introducing of nano-clays into hydrogels compositions can be considered as one of the methods to improve this property of superabsorbents [11]. It has been reported that inclusion of nano-clays in the hydrogel composition not only their strength can improve but also the rate and dye adsorption capacity will be increased [12]. Nanocomposites superabsorbents containing Na-montmorillonite [13], laponite [14], attapulgite [15], and sepiolite [16] have been synthesized and used to remove pollutions from aquatic media. Also, due to non-toxicity and biodegradability of biopolymers, the removal of dyes from water has been assessed by using nanocomposite superabsorbents based on polysaccharides biomass [17].

Because of eco-friendly property of carrageenan with  $\text{SO}_3^-$  groups (Scheme 1), we attempted to synthesize nanocomposite superabsorbents by introducing of this biopolymer. The current work describes the synthesis of crosslinked poly (sodium acrylate-co-acrylamide) in the presence of carrageenan biopolymer and sodium montmorillonite nano-clay. The structures of nanocomposite superabsorbents were investigated using FTIR, XRD, and SEM technique. The effect of reaction variables on the water absorbency of nanocomposites was studied. The capability of the so-obtained nanocomposite superabsorbents was examined to remove cationic crystal violet dye from water. Cationic crystal violet, an aromatic amine, is used to dye paper, ink industry, and others. The aromatic amines are highly carcinogenic that make it important to remove crystal violet from wastewater before discharging it to environment.

## Experimental

### Materials

*kappa*-Carrageenan (Carra) was obtained from Condinson Co., Denmark. N,N-methylenebisacrylamide (MBA) and potassium persulfate (KPS) from Fluka, and acrylamide



**Scheme 1** Structure of carrageenan biopolymer

**Table 1** Feed compositions for the synthesis of nanocomposite hydrogels. (KPS 0.1 g, MBA 0.1 g, T 60 °C, Water 30 mL)

	Clay0	Clay5	Clay10	Clay14	Clay18	Carra0	Carra5	Carra10	Carra14	Carra18	AAm0	AAm25	AAm50	AAm75	AAm100
Clay (g)	0	0.25	0.5	0.75	1	0.5	0.5	0.5	0.5	0.5	0.5	0.5	0.5	0.5	0.5
Carrageenan (g)	0.5	0.5	0.5	0.5	0.5	0	0.25	0.5	0.75	1	0.5	0.5	0.5	0.5	0.5
AAm+AA (g)	2+2	2+2	2+2	2+2	2+2	2+2	2+2	2+2	2+2	2+2	0+4	1+3	2+2	3+1	4+0

(AAM) from Rotterdam, the Netherlands, were of analytical grade and were used as received. Acrylic acid (Merck) was used without further purification. Natural sodium-montmorillonite (sodium Cloisite, Na-MMt) as a clay with cation exchange capacity of 92 meq/100 g of clay was provided by Southern Clay Products. All other ingredients were analytical grades and were used as received.

#### Synthesis of nanocomposite superabsorbents

The feed compositions for the synthesis of nanocomposite hydrogels are summarized in Table 1. The suffix *m* and *n* in Clay<sub>*m*</sub>, Carra<sub>*n*</sub>, and are wt% of Clay and Carra in nanocomposite composition, and suffix *z* in AAm<sub>*z*</sub> is wt% of acrylamide in monomer feed. In general, clay was dispersed in 30 mL of distilled water and stirred under magnetic stirrer for 24 h. Dispersed clay solution was transferred in a one-liter reactor equipped with mechanical stirrer. To control the reaction temperature, the reactor was placed in a water bath preset at 60 °C. Then, carrageenan was added to the solution containing clay and stirred for 2 h until completion of dissolution. AA was neutralized up to 80 % neutralization using NaOH 10 wt% at 0 °C, and AAm and MBA were dissolved in neutralized acrylic acid (e.g. sodium acrylate,

Na-AA) and were simultaneously added into polymerization solution and allowed to stir for 1 h. Finally, KPS (0.1 g in 2 mL of water) as initiator was added into solution and stirred until superabsorbents formation. After this time, the nanocomposites were dried at ambient temperature for 1 week. The dried samples were milled and sieved to 40–60 mesh sizes and kept away from light and moisture.

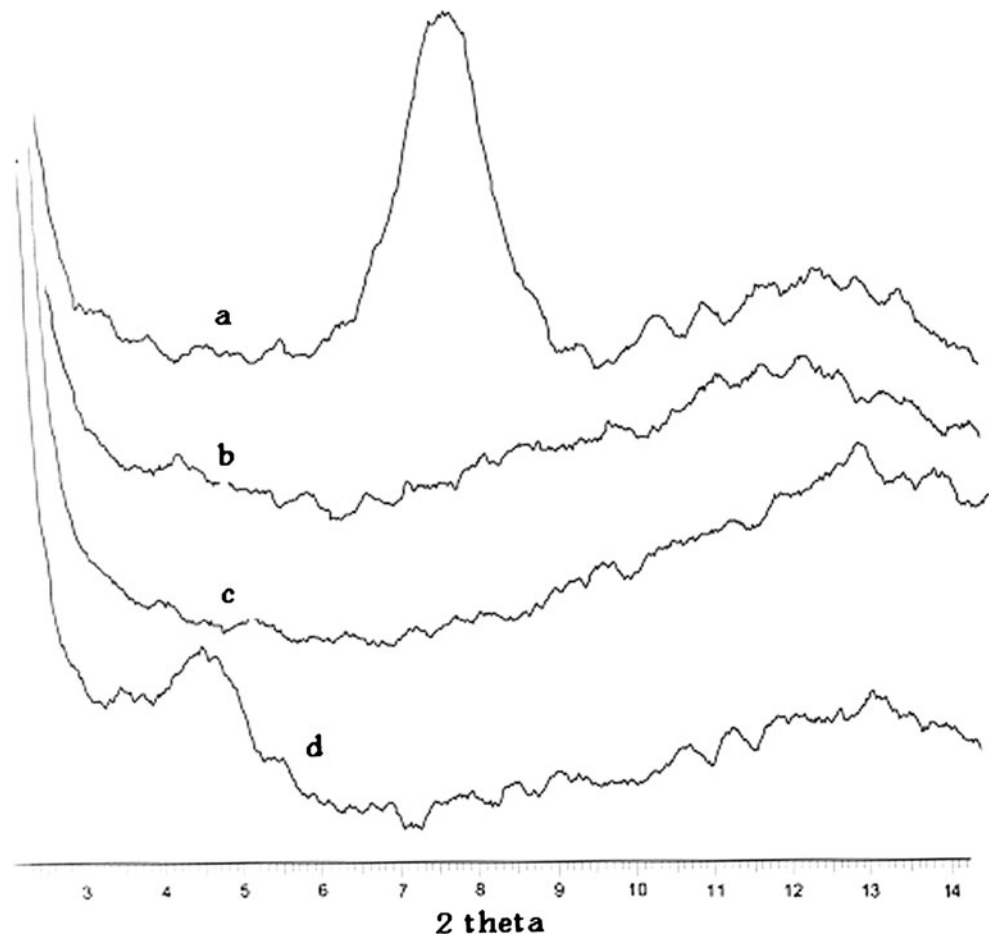
#### Swelling measurements

Dried nanocomposites were used to determine the degree of swelling. The degree of swelling (DS) was determined by immersing the nanocomposite superabsorbents (0.1 g) in distilled water (100 mL) and was allowed to soak for 24 h at room temperature. After this time, they were removed from the water, blotted with filter paper to remove surface water, weighed and the DS (g water/g dried nanocomposite) was calculated using Eq. (1):

$$DS = \frac{W_s - W_d}{W_d} \quad (1)$$

where  $W_s$  and  $W_d$  are the weights of the samples swollen in water and in dry state, respectively.

**Fig. 1** XRD profiles of a pristine clay and nanocomposites containing b 5, c 10, d 14 wt% of Na-MMt



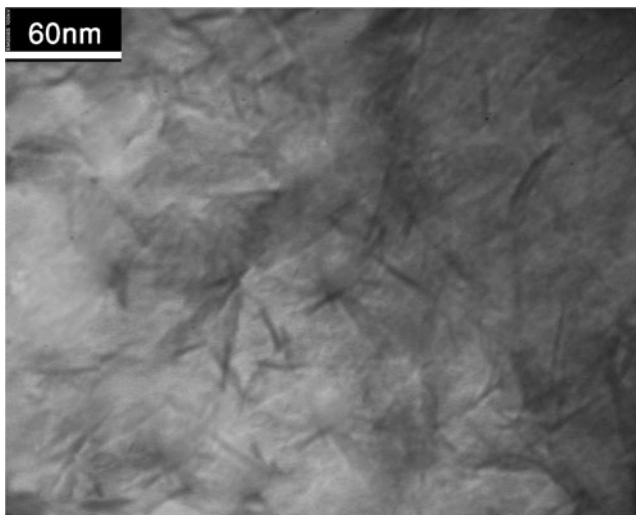


**Fig. 2** TEM image of Clay10 nanocomposite

#### Gel content

To estimate the un-reacted residual monomer and materials than can not participated in nanocomposite composition, 0.2 g of nanocomposites was immersed in distilled water for 72 h, and then swollen nanocomposites were filtered, dewatered with 200 ml ethanol and dried at 70 °C for 5 h.

Dried samples weighed and gel content (*Gel %*) was calculated by Eq. 2.

$$Gel\% = \frac{m}{M} \times 100 \quad (2)$$

where, *m* and *M* stand for final and initial weight of the sample, respectively.

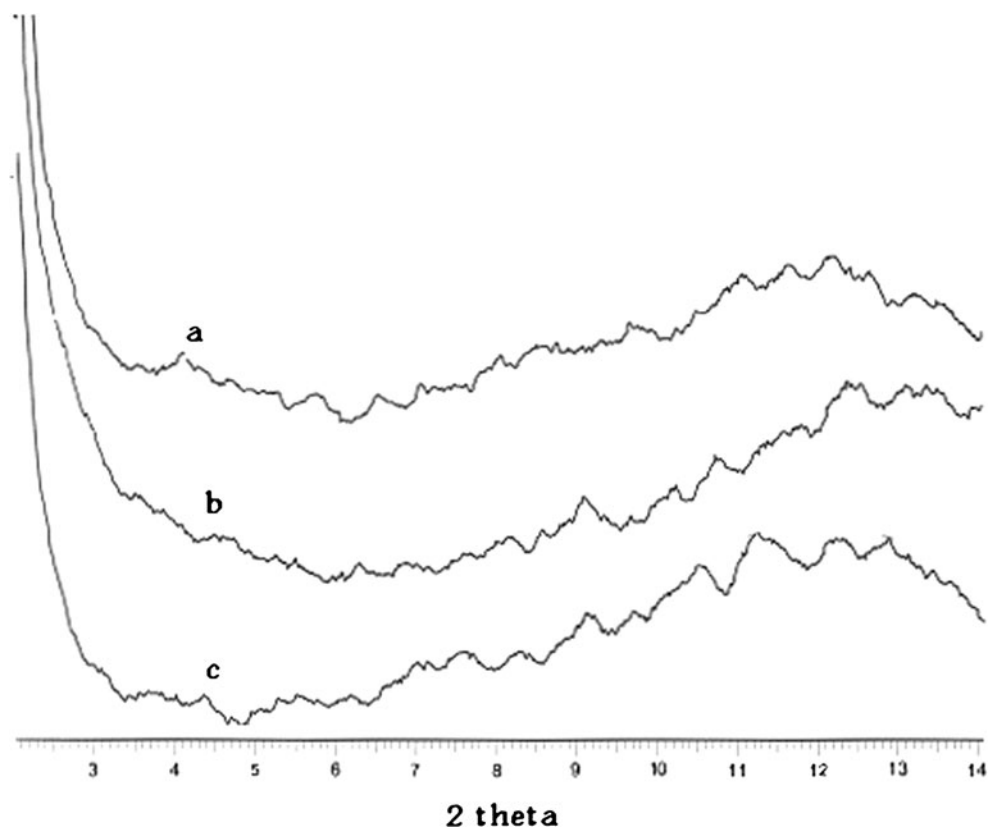
#### Dye adsorption measurements

Dye adsorption was carried out by immersing the 0.05 g of nanocomposites into 50 mL of dye solution with 30 mg/L of CV solution. All adsorption experiments were examined through a batch method on a stirrer with a constant speed at 120 rpm. To study the adsorption kinetics, at specified time intervals, the amount of adsorbed CV was evaluated using a UV spectrometer at  $\lambda_{max}=590$  nm. The content of adsorbed dye was calculated using following Eq. 3:

$$q_t = \frac{(C_0 - C_t)}{m} \times V \quad (3)$$

where,  $C_0$  is the initial CV concentration (mg/L),  $C_t$  is the remaining dye concentrations in the solution at time *t*, *V* is the volume of dye solution used (L), and *m* (g) is the weight of nanocomposite. Adsorption isotherm was carried out by

**Fig. 3** XRD patterns of nanocomposites containing **a** 0 wt% of Na-AA, **b** 1:1 weight ratio of monomers, and **c** 100 wt% of Na-AA



immersing of 0.05 g of nanocomposites into 50 mL of dye solutions with 10, 20, 30, 40, and 50 mg/L of CV for 24 h. The equilibrium adsorption capacity of nanocomposites,  $q_e$  (mg/g), was determined using Eq. 3. At this Eq., the  $C_i$  and the  $q_i$  will be replaced with equilibrium concentration of dye in the solution ( $C_e$ ) and equilibrium adsorption capacity ( $q_e$ ), respectively.

The removal efficiency ( $RE$  %) of CV by nanocomposites was calculated as follows:

$$RE\% = \frac{C_0 - C_e}{C_0} \times 100 \quad (4)$$

where,  $C_e$  is the remaining CV concentration in the solution.

#### Instruments

Dried nanocomposite was coated with a thin layer of gold and imaged in a SEM instrument (Vega, Tescan). One-

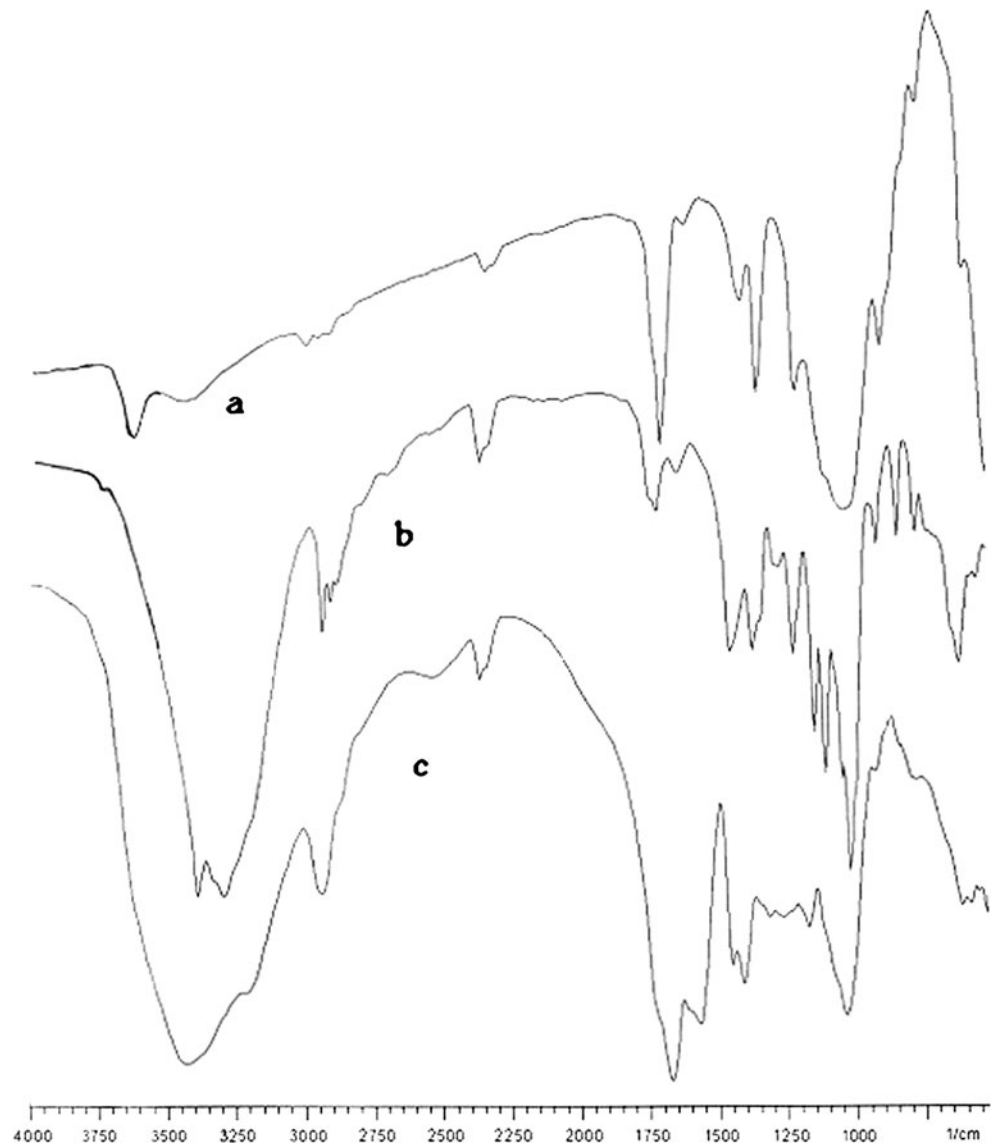
dimensional, wide angle X-ray diffraction patterns were obtained by using a Siemens D-500 X-ray diffractometer with wavelength,  $\lambda=1.54 \text{ \AA}$  (Cu-K $\alpha$ ), at a tube voltage of 35 KV, and tube current of 30 mA. The FTIR spectra were performed using ABB Bomem spectrophotometer (KBr pellets). TEM micrographs were recorded with a Philips CM10 operating at 60 kV tension.

## Results and discussion

### Synthesis and characterization

Nanocomposite superabsorbents were prepared by simultaneously copolymerization of Na-AA and AAm in the presence of carrageenan backbones and using the MBA and sodium MMT as crosslinker and nanoclay. KPS was used

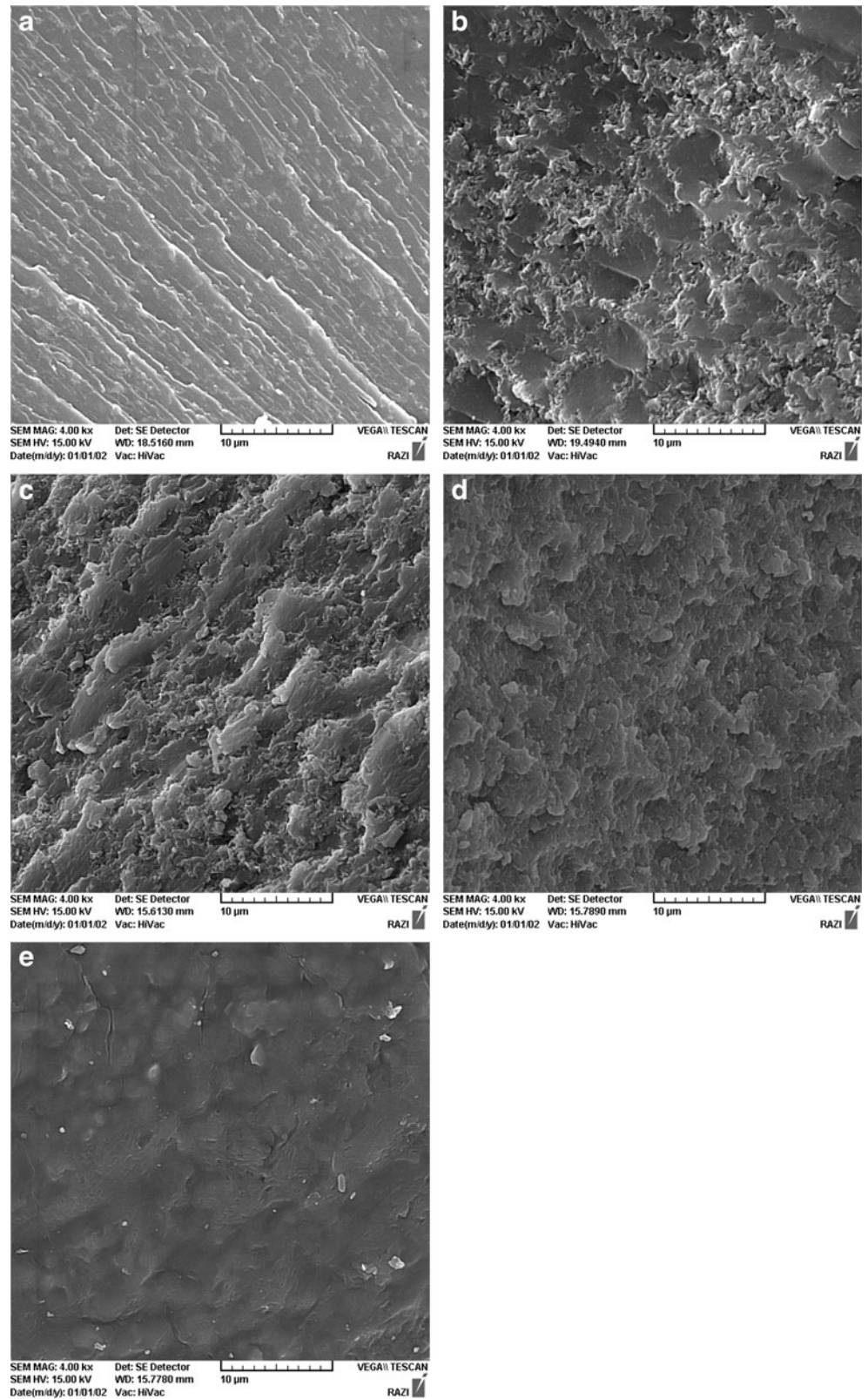
**Fig. 4** FTIR of a pristine clay b carrageenan and c Clay10 nanocomposite



as initiator. The persulfate initiator can decompose under heating and the resultant radicals will cause simultaneously copolymerization of Na-AA and AAm monomers. In the

presence of a cross-linker, i.e. MBA, cross-linking reaction can occur and finally a three dimensional network is produced. The carrageenan biopolymer can not intercalate into

**Fig. 5** SEM micrographs of **a** clay-free hydrogels, **b** Clay5, **c** Clay10, **d** Clay18, and **e** AAm0 nanocomposites



Na-MMt layers because of its anionic character. But, it will be captured between crosslinked poly (sodium acrylate-co-acrylamide) and Na-MMt networks and subsequently, a semi-IPN nanocomposite hydrogel will be formed.

The type of dispersion of nanoclay in the superabsorbents matrix was studied using XRD and TEM techniques. The XRD patterns of nanocomposites as a function of clay and monomer ratios were shown in Figs. 1 and 3. The XRD profile of pristine Na-MMt (Fig. 1a) imply a strong diffraction peak at  $2\theta=7.6$  corresponding to the distance of clay sheets with d spacing 11.61 Å. By varying the clay content up to 10 wt% (Fig. 1), although it seems that there is no diffractive peak, because of strong noises, it was difficult to conclude the exfoliation or intercalation of Na-MMt nanoclay in polymer matrix. So, we investigated the TEM image of Clay10 and the result was shown in Fig. 2. According to this figure, the MMt clay exists in both exfoliation and intercalation forms. When the clay content was 14 wt% (Fig. 1d), a diffractive peak ( $2\theta=4.3$ ) was observed and indicates that the intercalation dominates.

The XRD profiles of nanocomposites containing 0 wt% of Na-AA (AAm100, Fig. 3a), 1:1 weight ratio of monomers (AAm50, Fig. 3b), and the superabsorbent containing only Na-AA monomer (AAm0, Fig. 3c) are depicted in Fig. 3. It is obviously seen that all samples show no distinct diffraction peak; but similar as clay series, the XRD patterns contain strong noises and it may be concluded that the clay dispersion in polymer matrix is in the form of exfoliation and intercalation together. However, nanocomposites hydrogels comprising Na-MMt nanoclay and Na-AA monomer have been reported and the XRD studies of related nanocomposites have showed exfoliated structures [18, 19].

The structure of Nanocomposites was studied using FTIR spectra. The spectra of pristine clay, carrageenan, and nanocomposite are illustrated in Fig. 4. In the pristine clay spectrum (Fig. 4a), the characteristic peaks at 3634, 3448,

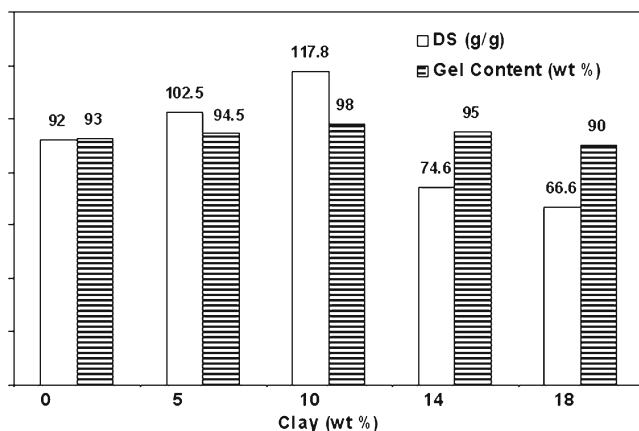


Fig. 6 Effect of clay content on the water absorbency and gel content of nanocomposites

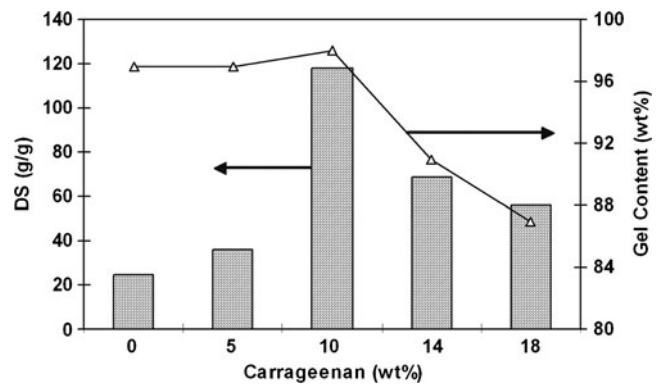


Fig. 7 Water absorbency and gel content of nanocomposites as a function of carrageenan content

1638 and  $1041\text{ cm}^{-1}$  are assigned to (–OH stretch from lattice hydroxyl, –OH stretch from free  $\text{H}_2\text{O}$ , –OH bending and Si–O stretch, respectively. The FTIR of carrageenan (Fig. 4b) shows characteristic bands at  $3000\text{--}3418$  and  $1373\text{ cm}^{-1}$  due to the of O–H and sulfate stretch, respectively. The peaks at  $1026, 918,$  and,  $841\text{ cm}^{-1}$  are attributed to the glycoside linkage, 3,6-anhydro-D-galactose, and C–O–S in galactose segments, respectively. The FTIR of nanocomposite Clay10 containing MMt, carrageenan, and poly (sodium acrylate-co-acrylamide) components was shown in Fig. 4c. As can be seen from the figure, the characteristic peak at  $3634\text{ cm}^{-1}$  correspondence to MMt disappeared and this observation shows the interaction of clay and polymer functional groups. The peak at  $1041\text{ cm}^{-1}$  due to Si–O stretch confirms the presence of clay in the nanocomposite composition. The presence of carrageenan component in the nanocomposite is confirmed by a peak at  $1319\text{ cm}^{-1}$  due to sulfate stretch. Comparing with pure carrageenan, this peak shows a shifting and may be attributed to the interaction of sulfate groups by other functional groups of nanocomposite. Poly (sodium acrylate-co-acrylamide) chains carry carboxamide and carboxylate functional groups. The Amide groups are

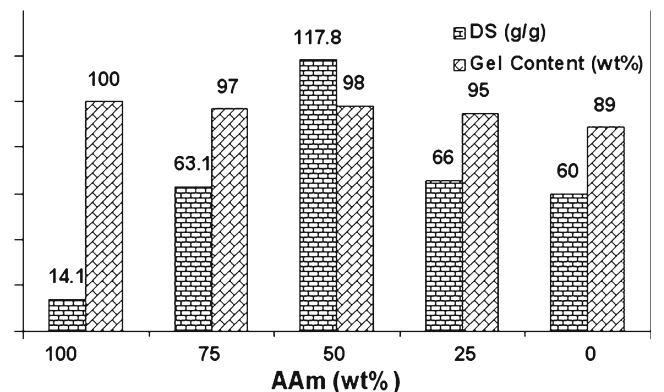
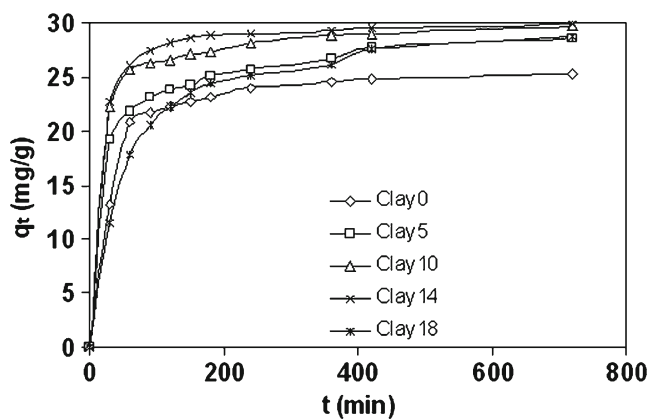


Fig. 8 Effect of monomer weight ratios on the water absorbency and gel content of nanocomposites



**Fig. 9** Dye adsorption speed of nanocomposites as a function of clay content (0.05 g of nanocomposites in 50 mL of dye solution with 30 mg/L of CV)

evidenced by peaks at  $1674\text{ cm}^{-1}$  due to the primary amides  $\text{-N-H}$  bending and  $3209\text{ cm}^{-1}$  corresponds to amide  $\text{-NH}$  symmetric stretching vibrations. The carboxylate groups are confirmed by the band characteristics at  $1574\text{ cm}^{-1}$  due to asymmetric stretching in carboxylate anion that is reconfirmed by another peak at  $1412\text{ cm}^{-1}$  which is related to the symmetric stretching mode of the carboxylate anion

One of the most crucial properties of nanocomposites which can be considered is hydrogel microstructure morphology. Figure 5 shows the SEM micrographs of clay-free hydrogel and nanocomposites. While the hydrogels without clay shows a relatively tight surface (Fig. 5a), the Caly5 and Clay10 nanocomposites (Fig. 5b and c) contain coarse and undulant surface. In comparing to Clay5 and Clay10, the surface roughness of Clay18 was decreased. Also, studying the micrograph of nanocomposites revealed that the surface morphology of nanocomposites depends on monomers ratios. The surface of AAm0 (Fig. 5e) in compared with nanocomposites containing 1:1 ratio of monomers (Fig. 5c) showed relatively smooth surface.

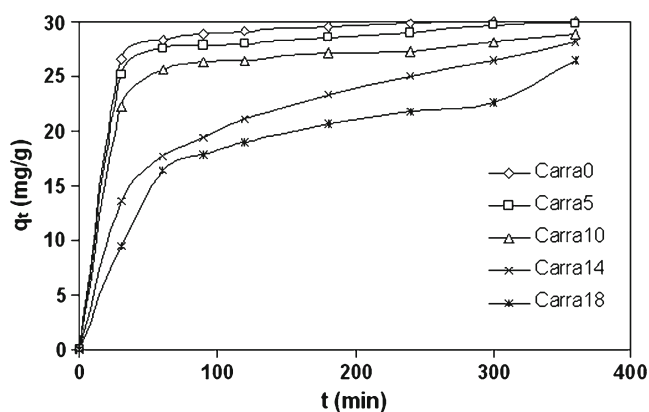
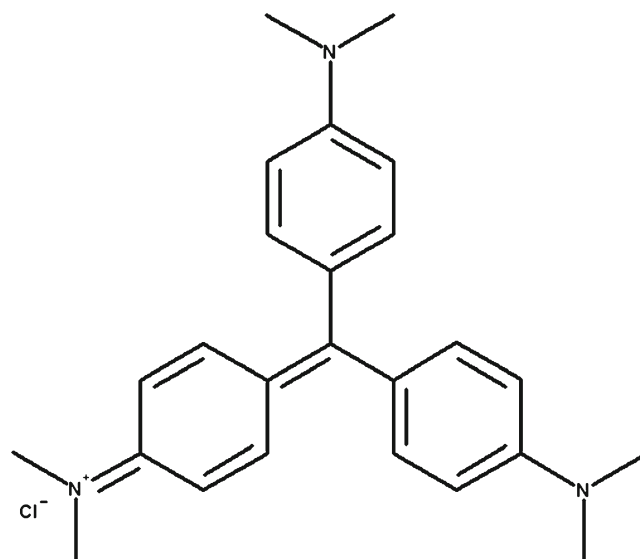


**Fig. 10** Dye adsorption speed of nanocomposites as a function of carrageenan content (0.05 g of nanocomposites in 50 mL of dye solution with 30 mg/L of CV)



**Scheme 2** Structure of crystal violet dye

### Swelling of nanocomposites

Degree of swelling of nanocomposites was investigated by changing the reaction variables including clay and carrageenan contents as well as the monomers weight ratios. Water absorbency of nanocomposites dependence on clay content is shown in Fig. 6. As it is evident from figure, by changing the clay content up to 10 wt% caused an increase in water absorbency of nanocomposites. Maximum water absorbency ( $117.8\text{ g/g}$ ) was obtained for nanocomposite with 10 wt% of Na-MMt nanoclay. In fact, increasing Na-MMt content up to 10 wt% improves water absorbency of nanocomposite. The corresponding increase in swelling up to 10 wt% of MMt could be attributed to increase in ionic osmotic pressure of nanocomposites. This osmotic pressure is due to the mobile ions on the nanoclay particles [20]. When the amount of Na-MMt in the nanocomposite

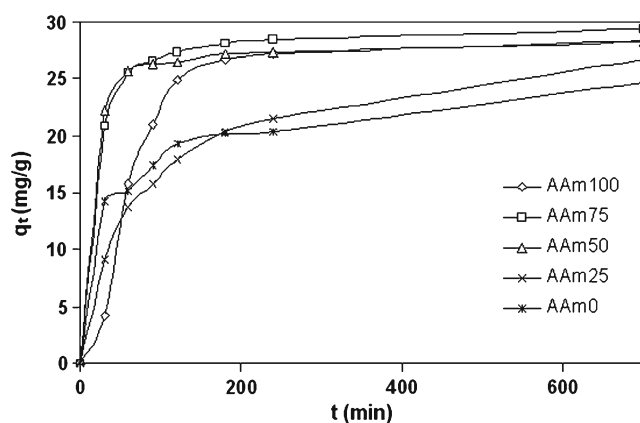


**Fig. 11** Dye adsorption speed of nanocomposites as a function of monomer weight ratios (0.05 g of nanocomposites in 50 mL of dye solution with 30 mg/L of CV)



composition was increased from 10 to 18 wt% of nanoclay, a decrease in water absorbency was found. The gel contents of nanocomposite containing different amounts of Na-MMT were determined and the results are shown in Fig. 6. The gel contents of Clay14 and Clay18 samples showed a decrease of 3 and 8 wt% compared with Clay10. By decreasing the gel content, swelling capacity will decrease. In fact, by further increase in Na-MMT content, the viscosity of polymerization medium will increase and restrict the macroradicals movement; thereby decreasing the gel content and subsequently, the water absorbency will decrease. The other reason to reduce in water absorbency by increasing of clay content can be attributed to act of nanoclay as

multifunctional crosslinker [21]. More crosslinking points causes the higher crosslinking density and decreases the space between the copolymer chains and consequently, the resulted highly crosslinked rigid structure cannot be expanded and hold a large quantity of water. A similar behavior have been reported by Al et al in the case of starch-g-acrylic acid/An-MMT nanocomposite hydrogels [22].

The swelling dependency of nanocomposites on carrageenan amount is shown in Fig. 7. The maximum water absorbency was obtained at 10 wt% of carrageenan, whereas others, including clay content and monomers ratio were kept constant. The increment in water absorbency of nanocomposites by increasing carrageenan content is attributed to the

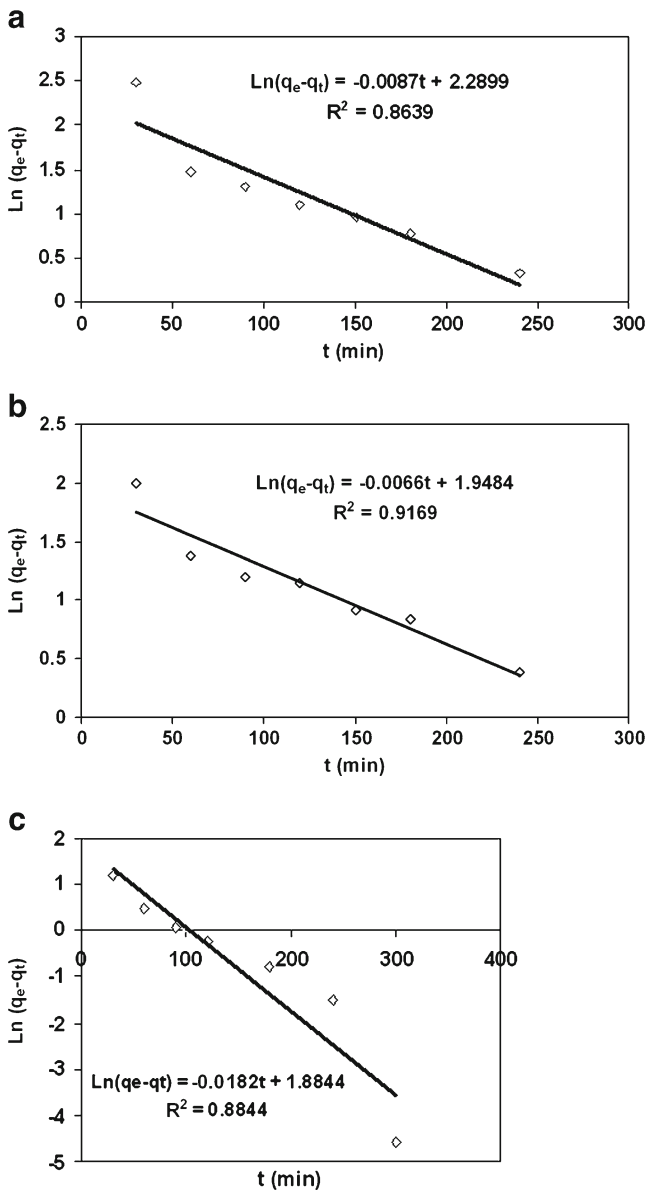


**Fig. 12** Adsorption kinetic of the CV onto the **a** clay-free hydrogel, **b** Clay10 nanocomposite, and **c** Carra0 nanocomposites according to pseudo-first-order model

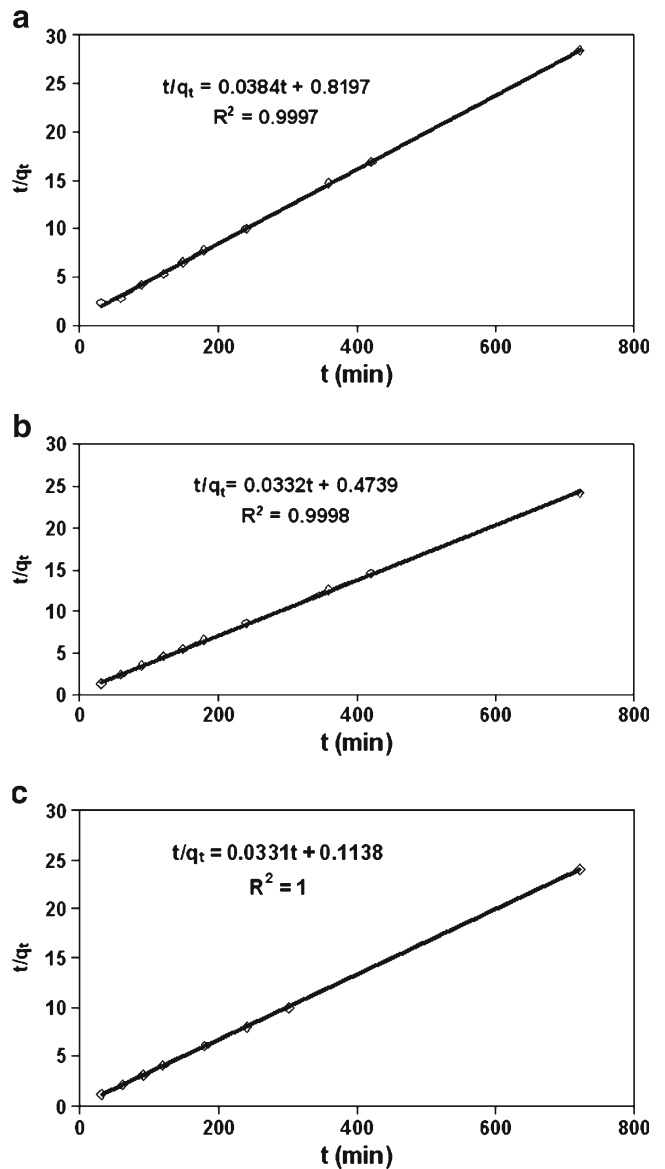


**Fig. 13** Adsorption kinetic of the CV onto the **a** clay-free hydrogel, **b** Clay10 nanocomposite, and **c** Carra0 nanocomposites according to pseudo-second-order model

enhancement of the ionic sulfate anions. The electrostatic repulsive force between the charged sites ( $-\text{SO}_3^-$ ) causes increasing in swelling. However, increases in carrageenan content above 10 wt% resulted in decreased absorbency. This decrease in water absorbency can be attributed to decrease in gel contents of nanocomposites due to increase in viscosity of the medium which hinders the movement of free radicals and monomer molecules. As shown in Fig. 7, above 10 wt% of carrageenan, the gel content was significantly decreased for Carra14 and Carra18 compared with Carra10.

Different nanocomposites with various AAm/Na-AA weight ratios were synthesized through changes in monomers ratio. The degree of swelling of the nanocomposites prepared with various ratios of monomers is shown in Fig. 8. It is observed that the water absorbency is significantly increased with decreasing AAm in the AAm/Na-AA ratio and then reduced. The initial increment in swelling values can be attributed to increase in ionic groups existing in copolymer chains along with increase of Na-AA in the nanocomposite which allows polymer coils to expand more easily. The swelling loss after the maximum may be originated from reducing the gel content due to the higher amount of Na-AA (Fig. 8). Also, according to Nazripour et al studies, in the copolymerization of AAm and Na-AA, the reactivity of Na-AA is lower than that of AAm monomer and subsequently, by increasing in Na-AA monomer ratio, the gel content will decrease [23]. As shown in Fig. 8, an AAm/Na-AA ratio of 50 % provides the best values of swelling (117.8 g/g).

## Dye adsorption studies

### Rate of adsorption and adsorption kinetics

The structural property of adsorbents is prominent parameter that can affect the adsorption speed of adsorbate onto adsorbents [24]. So, we tried to investigate the dye adsorption speed of nanocomposites as a function of reaction variables. The influences of the clay and carrageenan contents as well as the AAm/Na-AA monomers ratios on dye adsorption speed of nanocomposites are shown in Figs. 9, 10, and 11. As it is clear from Fig. 9, the clay content can affect the rate of the dye adsorption onto nanocomposites. In fact, inclusion of Na-MMt nanoclay into carrageenan-based hydrogel caused an enhancement in dye adsorption speed. Because of negative centers on the Na-MMt nanoclay, the negative charge density enhances as the clay content increases in the nanocomposite composition. Enhancement in negative charge density on the nanocomposite increases the chance of collisions with cationic dye and subsequently, the rate of dye adsorption will increase [25]. Although the water absorbency of nanocomposites was increased up to 10 wt% of nanoclay, the increment in dye adsorption speed was observed up to 14 wt% of Na-MMt. Decreasing of the dye adsorption speed of CV onto nanocomposite with 18 wt% of Na-MMt nanoclay, can be attributed to the low swelling capacity of nanocomposite.

Figure 10 indicates dye adsorption speed dependence on the carrageenan content of nanocomposites in solution containing 30 mg/g of CV. Carrageenan is a biopolymer

**Table 2** The pseudo first-order and pseudo second-order rate parameters for CV adsorption by nanocomposites

	First-order kinetics				Second-order kinetics			
	$q_e$ , Theor., mg/g	$q_e$ , Exp., mg/g	$K_1 \times 10^3$ , g/mg.min	$R^2$	$q_e$ , Theor., mg/g	$q_e$ , Exp., mg/g	$K_2 \times 10^3$ , $\text{min}^{-1}$	$R^2$
Clay0	6.7	25.3	8.7	0.8639	26.5	25.3	1.2	0.9997
Clay5	6.15	28.54	4.7	0.9643	29.3	28.54	1.04	0.9991
Clay10	5	29.66	6.6	0.9169	30.1	29.66	0.52	0.9998
Clay14	3.45	29.83	6.5	0.874	30.2	29.83	0.33	1
Clay18	9.51	28.7	9.51	0.9324	30.4	28.7	1.6	0.9993
Carra0	4.7	30	18.2	0.8844	30.2	30	0.124	1
Carra5	4.2	29.9	10	0.8505	30.2	29.9	0.265	0.9998
Carra10	5	28.85	6.6	0.9169	30.1	28.85	0.52	0.9998
Carra14	10.94	29.66	7.6	0.991	26.88	29.66	1.36	0.9976
Carra18	9.48	26.5	4.9	0.917	28.4	26.5	2.6	0.9991
AAm0	7.44	28.3	4.6	0.8744	25.5	28.3	1.52	0.9973
AAm25	11.2	29.38	5.6	0.9526	29.1	29.38	1.17	0.9969
AAm50	5	29.66	6.6	0.9169	30.1	29.66	0.52	0.9998
AAm75	7.5	26.67	7.5	0.9124	29.8	26.67	1.12	1
AAm100	16.3	24.66	1.47	0.9447	32.5	24.66	0.94	0.9986

carrying anionic sulfonate groups. It was expected that like clay series, the rate of dye removal can increase due to negative  $-SO_3^-$  groups. But on comparing with clay series, the results were obtained in inverse direction. During 1 h, the  $RE\%$  for the nanocomposite without carrageenan component was about 94 %. In contrast, at this time, the amount of dye adsorption was lower in order of Carra5 (91.2 %), Carra10 (85.5 %), Carra14 (58 %), and Carra18 (54 %). The decrease in rate of adsorption of nanocomposite with increasing of carrageenan may be attributed to high hydrophilic property of carrageenan. This property of carrageenan hinders the ease of nearing of cationic dye with the large hydrophobic segment (Scheme 2).

Because of anionic property of sodium acrylate monomer, we endeavored to study the dye adsorption speed dependence on monomer ratio. Due to negative charge of Na-AA monomer, increasing this component in monomer feed up to 50 wt% caused an enhancement in dye adsorption speed (Fig. 11). Despite the enhancement of negative charge density by increasing Na-AA monomer in nanocomposite composition, the dye adsorption speed decreased above 50 wt% of Na-AA in monomer feed. Reduction in dye adsorption speed may be attributed to the corresponding low swelling capacity of nanocomposites as the Na-AA monomer ratio is increased from 50 to 100 wt%.

Studying of adsorption kinetics represents the pollutant adsorption rate, which dominates the time of adsorbate adsorption at the solid-liquid surface [15]. In fact, kinetic of adsorption is one of the most factors for finding the efficiency of adsorption. Pseudo-first-order and pseudo-second-order kinetic models were examined to obtain rate constant and equilibrium adsorption capacity for all nanocomposite samples. So, kinetic data were analyzed by using the pseudo-first-order equation as below [26]:

$$\ln(q_e - q_t) = \ln q_e - k_1 t \tag{5}$$

where,  $q_e$  and  $q_t$  (mg/g) are the amount of adsorbed dye on the nanocomposites at equilibrium and at time  $t$ , respectively.  $k_1$  ( $\text{min}^{-1}$ ) presents the rate constant of first-order adsorption. In order to obtain model calculations  $k_1$  and  $R^2$  (correlation coefficient), we can plot  $\ln(q_e - q_t)$  against  $t$  for Pseudo-first-order (Fig. 12).

Also, kinetic data were analyzed by using the second-first-order equation as below [26]:

$$\frac{t}{q_t} = \frac{1}{k_2 q_e^2} + \frac{t}{q_e} \tag{6}$$

here,  $k_2$  (g/mg.min) is rate constant of second-order adsorption and  $q_e$  is the theoretical adsorbed dye (mg/g) that can be calculated from pseudo-second-order. In order to obtain model calculations  $k_2$  and theoretically equilibrium adsorption ( $q_e$ ) as well as  $R^2$  (correlation coefficient), we can  $\frac{t}{q_t}$  against  $t$

(Fig. 13). Model calculations for all nanocomposites were given in Table 2. It was found that the plotting of  $\frac{t}{q_t}$  against  $t$  gives a straight-line with a high correlation coefficient ( $R^2 > 0.99$ ) and it can be concluded that adsorption kinetic of dye by all nanocomposites has the best fitting to the pseudo-second-order. As can be seen from the data, according to pseudo-second-order kinetic, and theoretical equilibrium adsorption capacities are in agreement with the experimental data.

Adsorption isotherms

In order to study adsorption isotherms, 0.05 g of selected nanocomposites (Clay0, Clay10, Carra0, AAm100, AAm50,

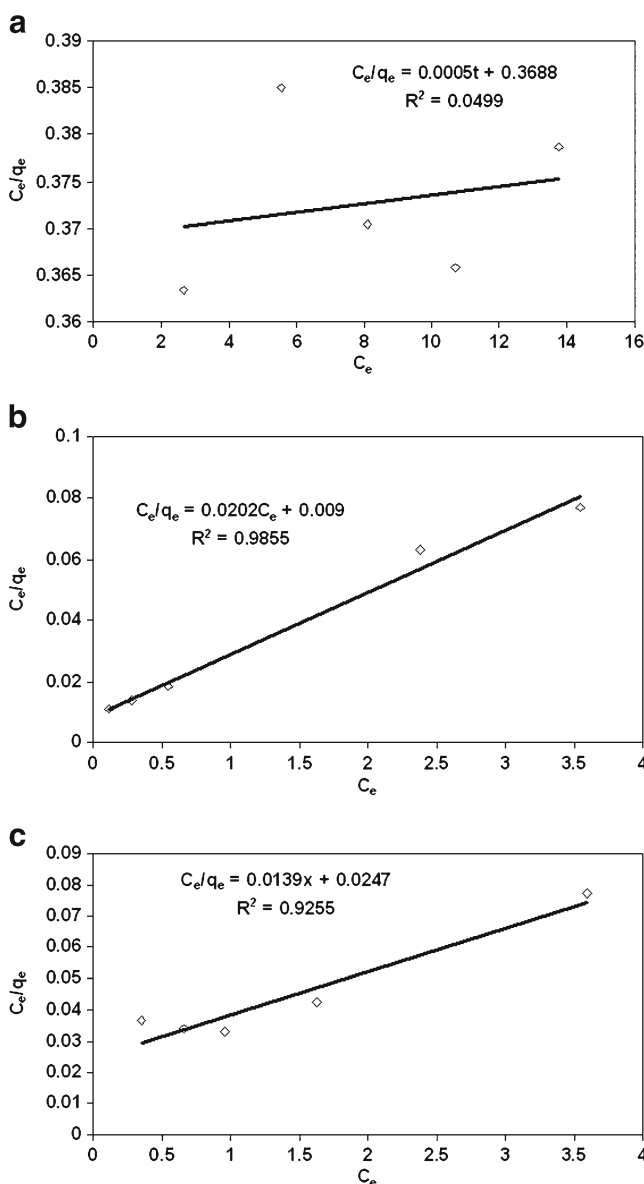
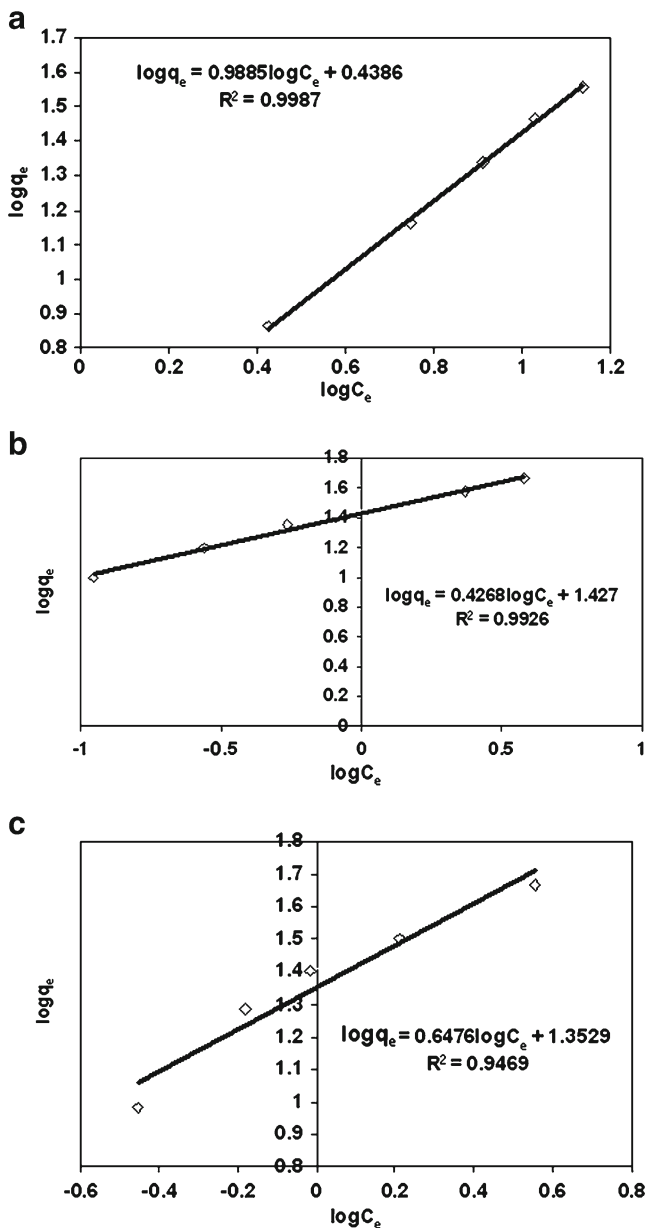


Fig. 14 Plot of Langmuir isotherm for the adsorption of CV onto a clay-free hydrogel, b Clay10 nanocomposite, and c Carra0 nanocomposites



**Fig. 15** Plot of Freundlich isotherm for the adsorption of CV onto **a** clay-free hydrogel, **b** Clay10 nanocomposite, and **c** Carra0 nanocomposites

and AAm0) were immersed into dye solutions with initial concentrations ranging from 10 to 50 mg/L. The adsorption isotherms describe the optimized adsorption system as well as the effectiveness of adsorbents. In fact, it is important to investigate to obtain an optimum isotherm model indicating the CV adsorption system onto nanocomposite hydrogels. The practical data were fitted to the Langmuir and Freundlich models. In the Langmuir adsorption model, adsorption of adsorbate takes place at specific homogeneous sites within the adsorbent and is valid for monolayer adsorption onto adsorbents [27]. The expression of the applied Langmuir model is given by the Eq. 7:

$$\frac{C_e}{q_e} = \frac{C_e}{q_m} + \frac{1}{q_m b} \quad (7)$$

where,  $C_e$  is the equilibrium dye concentration in the solution (mg/L),  $b$  is the Langmuir adsorption constant (L/mg), and  $q_m$  is the theoretical maximum adsorption capacity (mg/g). The  $q_m$  and  $b$  can be calculated from the slope and intercept of a linear plot of  $\frac{C_e}{q_e}$  versus  $C_e$ , respectively (Fig. 14).

In the Freundlich model, the adsorption of adsorbate occurs on a heterogeneous surface by multilayer sorption and the adsorption capacity can increase with an increase in adsorbate concentration [25, 27]. Freundlich isotherm is represented by the following equation:

$$\log q_e = \log k_f + \frac{1}{n} \log C_e \quad (8)$$

where,  $K_f$  is the equilibrium adsorption coefficient (L/g), and  $1/n$  is the empirical constant. The  $K_f$  and  $n$  values for nanocomposites can be achieved from the intercept and the slope of plotting  $\log q_e$  against  $\log C_e$  (Fig. 15). In fact, the  $n$  value depicts the favorability of adsorption process and  $k_f$  is the adsorption capacity and intensity of the adsorbate.

The all expressions in Langmuir and Freundlich equations and equilibrated adsorption of all nanocomposites were calculated according to experimental data and summarized in Table 3. In accordance with the high correlation coefficient in Freundlich equation ( $R^2 > 0.94$ ), it depicts that

**Table 3** Isotherm parameters for adsorption of CV onto selected nanocomposites

Isotherm	Parameters	Samples						
		Clay0	Clay10	Carra0	Carra18	AAm100	AAm50	AAm0
Freundlich model	$n$ , g/L	1.01	2.34	1.54	1.87	1.28	2.34	3.73
	$K_f$ , mg/g	2.7	26.7	22.3	12.3	7.3	26.7	17.6
	$R^2$	0.9885	0.9926	0.9469	0.9507	0.9693	0.9926	0.9609
Langmuir model	$q_m$ , mg/g	2000	49.5	71.9	93	135.1	49.5	38.3
	$b \times 10^{-3}$ , L/mg	0.184	0.187	0.343	1.32	1.28	0.187	1.08
	$R^2$	0.0499	0.9855	0.9255	0.3593	0.0524	0.9855	0.9999
$q_e$ (Exp), mg/g		36.2	46.15	46.4	41.18	42.8	46.15	34.7

Freundlich isotherm is the best fit of experimental data than the Langmuir model. Considering the results, it is concluded that the adsorption of CV onto nanocomposites take places through heterogeneous surface by multilayer sorption. In Freundlich model, when  $n$  values being between 1 and 10, the removing process will be beneficial adsorption [28]. The  $n$  values for all nanocomposites is bigger than 1 and indicate that Freundlich model is favorable for this system. Also, the  $k_f$  values for nanocomposites are comparable. While the  $k_f$  value of clay-free hydrogel is 2.7, it was increased as the nanoclay was introduced into carrageenan-based hydrogel. The  $k_f$  value of nanocomposite without carrageenan was 22.3 and the maximum  $k_f$  (26.7) was obtained for Clay10 nanocomposite comprising both clay and carrageenan components. In fact, the improvement of adsorbate intensity onto nanocomposites can achieve by simultaneously incorporation of nanoclay and carrageenan in nanocomposite composition. Also, according to  $k_f$  values, the maximum dye uptake will take place by simultaneously presence of AAm and Na-AA. The experimental equilibrium adsorptions of nanocomposites are illustrated in Table 3 and according to the results, the maximum dye adsorption capacity was observed for Carra0 nanocomposite with 46.4 mg/g adsorption capacity.

## Conclusions

Sodium montmorillonite was introduced into carrageenan-based hydrogels to improve water absorbency and the resultant nanocomposites were applied for removing CV cation dye from water. The results of the study are as below:

- According to XRD and TEM studies, the type of clay dispersion in nanocomposite matrix was exfoliation and intercalation forms up to 10 wt% of Na-MMt. According to XRD pattern, above 10 % of nanoclay, intercalation type was dominated. By varying the monomers ratios, the type of dispersion of nanoclay was not changed and it was exfoliated. The SEM micrographs showed that inclusion of Na-MMt can cause porous surface.
- Water absorbency capacity of nanocomposites was studied by changing the reaction variables. An increment in water absorbency was observed up to 10 wt% of Na-MMt due to mobile ions in the nanoclay that can cause an increase in osmotic pressure. At high content of nanoclay, the water absorbency was decreased that can be attributed to the acting of nanoclay as multifunctional crosslinker. Optimum water absorbency was achieved at 10 wt% of carrageenan and 1:1 weight ratio of AAm/Na-AA monomers.
- The obtained nanocomposites were examined to remove of CV dye from water. The results showed that the speed of dye removal can affect by clay and carrageenan content as well as monomers ratios. While the speed of dye removal was increased up to 14 wt% of nanoclay, the rate of dye removal was decreased as the carrageenan content was increased. Enhancement in dye adsorption speed was observed when the AAm amount in AAm/Na-AA ratios was increased up to 50 wt%.
- The results showed that the pseudo-second-order adsorption kinetic was predominated for the adsorption of CV onto nanocomposites.
- Freundlich model was obtained as the best model for the adsorption of CV onto nanocomposites.

## References

1. Eshel H, Dahan L, Dotan A, Dodiuk H, Kenig S (2008) Polym Bull 61:257
2. Po R (1994) J Macromol Sci Rev Macromol Chem Phys C34:607
3. Kost J (1999) In: Mathiowitz E (ed) Encyclopedia of controlled drug delivery. Wiley, New York
4. Bulut Y, Akcay G, Elma D, Serhatli IE (2009) J Hazard Mater 171:717
5. Hamidi M, Azadi A, Rafiei P (2008) Adv Drug Deliv Rev 60:1638
6. Jiuhui Q (2008) J Environ Sci 20:1
7. Ahmad R, Kumar R (2011) Clean-Soil Air Water 39:74
8. Sarri MM (2010) Water Sci Technol 61:2097
9. Karadag E, Saraydin D, Guven O (1996) J Appl Polym Sci 61:2367
10. Dutta PK, Dutta J, Tripathi VS (2004) J Sci Ind Res 63:20
11. Haraguchi K (2007) Curr Opin Solid State Mater 11:47
12. Liu P, Zhang L (2007) Sep Purif Technol 58:32
13. Dalaran M, Emik S, Guclu G, Iyim TB, Ozgumus S (2009) Polym Bull 63:159
14. Li P, Siddaramaiah, Kim NH, Yoo GH, Lee JH (2009) J Appl Polym Sci 111:1786
15. Liu Y, Wang W, Jin Y, Wang A (2011) Sep Purif Technol 46:858
16. Ekici S, Isikver Y, Saraydin D (2006) Polym Bull 57:231
17. Abou-Taleb MF, Hegazy DE, Ismail SA (2012) Carbohydr Polym 87:2263
18. Liu PS, Li L, Zhou NL, Zhang J, Wei SH, Shen J (2006) J Appl Polym Sci 102:5725
19. Wang W, Wang A (2009) J Compos Mater 43:2805
20. Li A, Zhang J, Wang A (2007) J Appl Polym Sci 103:37
21. Darvishi Z, Kabiri K, Zohuriaan-Mehr MJ, Morsali A (2011) J Appl Polym Sci 120:3453
22. Al E, Guclu G, Iyim TB, Emik S, Ozgumus S (2008) J Appl Polym Sci 109:16
23. Nazaripour S, Rafizadeh M, Bouhendi H (2012) e-Polymers no.017
24. Tsai WT, Lai CW, Hsien KJ (2003) J Colloid Interface Sci 263:29
25. Abdel-Halim ES, Al-Deyab SS (2011) Carbohydr Polym 86:1306
26. Zhu X, Jiang X, Cheng S, Wang K, Mao S, Fan LJ (2010) J Polym Res 17:769
27. Ansari R, Banimahd-Keivani M, Fallah-Delavar A (2011) J Polym Res 18:1931
28. Kadirvelik K, Namasivayam C (2000) Environ Technol 21:1091